

## Regular and stochastic acceleration of photons

J. T. Mendonça and L. Oliveira e Silva

*Centro de Electrodinâmica, Instituto Superior Técnico, Lisboa 1096 Codex, Portugal*

(Received 24 May 1993)

The Hamiltonian formulation of ray tracing trajectories is used to describe the various mechanisms of photon acceleration. This leads to a straightforward derivation of the frequency shifts and of the time and length scales. The existence of three types of photon trajectories, in the presence of an ionization front, is demonstrated. A threshold condition for transition from regular to stochastic photon acceleration is also derived.

PACS number(s): 52.40.Nk, 05.45.+b, 52.75.Ms

Generation of tunable radiation by laser-plasma interaction is presently a subject of growing interest. This is mainly motivated by the existence of experimental techniques for pulse compression, leading to fluxes larger than  $10^{18}$  W/cm<sup>2</sup> of laser radiation.

There are mainly two different mechanisms providing tunable radiation by laser-plasma interaction. One consists of reflection of a light pulse by a relativistic front, traveling with a velocity  $v \simeq c$ . This was first considered by Semenova and by Lampe, Ott, and Walker [1] and studied more recently by others [2]. The ionization front can be produced by a second light pulse, through photoionization. The frequency of the reflected pulse is upshifted by a factor  $(1+\beta)/(1-\beta)$ , with  $\beta=v/c$ , as in the case of a relativistic mirror.

The second mechanism results from the nonlinear interaction of two light pulses in a fully ionized and stationary plasma. In this case, the frequency shifting can be considered as an adiabatic process occurring along the pulse interaction, and it can result from the nonlinear changes of the plasma dispersion properties [3] or from the electron-density modulations associated with the plasma wave wake field [4].

In the present work, we will examine both mechanisms using the Hamiltonian formulation of photon or ray tracing equations. This approach will prevent us from examining partial reflection and the zero-frequency magnetic mode [12], which are nearly absent in present photon acceleration experiments anyway [5], but it will provide a simple and straightforward calculation of the space-time evolution of the photon frequency. A number of important qualitative features of ray tracing dynamics will also be described. In particular, the existence of three classes of ray trajectories, which were recently suggested by Mori [2] and by Yu *et al.* [6], will be topologically demonstrated here. We will also be able to show that a transition to stochastic photon acceleration can eventually occur, in the presence of two plasma wave wake fields, leading to a large frequency spread.

Strictly speaking, photon acceleration was initially proposed by Wilks *et al.* [4] to label the frequency shift produced by the wake field. But it will be used here as the equivalent of a frequency shift, because there are really no significant physical differences between the two above mentioned mechanisms, at least in the ray tracing approach.

We start with the well-known ray tracing equations [7] describing the evolution of a wave packet (which is the classical analog of a photon) in a slow space and time varying plasma. These equations can be written in Hamiltonian form, where the canonical variables are the photon position  $\mathbf{r}$  and wave vector  $\mathbf{k}$ , and the Hamiltonian is the photon frequency  $\omega \equiv \omega(\mathbf{r}, \mathbf{k}, t)$  as determined by the plasma dispersion relation. We assume here an unmagnetized plasma, with electron density perturbations moving with velocity  $\mathbf{v}$ . We then make a canonical transformation to the new variables  $\boldsymbol{\eta} = \mathbf{r} - \mathbf{v}t$ , and  $\mathbf{p} = \mathbf{k}$ , through the generating function  $F_2(\mathbf{r}, \mathbf{p}, t) = \mathbf{p} \cdot (\mathbf{r} - \mathbf{v}t)$ . The resulting canonical equations are

$$\frac{d\boldsymbol{\eta}}{dt} = \frac{\partial \Omega}{\partial \mathbf{p}}, \quad \frac{d\mathbf{p}}{dt} = -\frac{\partial \Omega}{\partial \mathbf{r}}, \quad (1)$$

where the Hamiltonian is now given by

$$\Omega(\boldsymbol{\eta}, \mathbf{p}, t) = \omega(\boldsymbol{\eta} \cdot \mathbf{p}) - \mathbf{v} \cdot \mathbf{p} = \sqrt{p^2 c^2 + \omega_p^2(\boldsymbol{\eta})} - \mathbf{v} \cdot \mathbf{p}. \quad (2)$$

Here we have assumed the cold plasma dispersion relation, which is valid for waves with phase velocities much larger than the electron thermal velocity. It is important to note that the new Hamiltonian is a constant of motion and can thus be determined by the initial conditions,  $\Omega = \omega_i - \mathbf{k}_i \cdot \mathbf{v}$ .

We will first examine the case where the electron-density perturbations are due to a plasma wave wake field in this case, we can write

$$\omega_p^2(\boldsymbol{\eta}) = \omega_{p0}^2 [1 + \epsilon f(\mathbf{k}_p \cdot \boldsymbol{\eta})], \quad (3)$$

where  $\omega_{p0}$  is the unperturbed electron plasma frequency and  $\mathbf{k}_p \simeq \mathbf{v}/\omega_{p0}$  is the plasma wave wave vector. The dependence of the amplitude  $\epsilon$  and the exact shape  $f(\mathbf{k}_p \cdot \boldsymbol{\eta})$  of the wake field cannot be related in a simple way to the intensity and shape of the driving laser pulse [8]. For the present purposes, we will then assume that  $\epsilon$  is arbitrary and  $f(\mathbf{k}_p \cdot \boldsymbol{\eta})$  is a periodic function of period  $2\pi/k_p$ , with a minimum value  $f^- = -a$ , and a maximum value  $f^+ = b$ . It will be shown below that the photon frequency shift is insensitive to the exact wake-field shape.

Let us now examine the photon dynamics described by Eqs. (1)–(3), restricting our analysis to the unidimensional case, where  $\mathbf{p}$  is parallel to  $\mathbf{k}_p$ . The periodic perturbation associated with the wake field will buildup, in phase space  $(\boldsymbol{\eta}, p)$ , a nonlinear resonance similar to that of an

asymmetric pendulum [9]. There will be an elliptic fixed point at  $(\eta = \pi/k_p; p = \gamma^2 \beta \Omega_0/c)$  and a hyperbolic fixed point at  $(\eta = 0, 2\pi/k_p; p = \gamma^2 \beta \Omega_x/c)$ , where  $\beta = V/c$  and  $\gamma = (1 - \beta^2)^{-1/2}$ . The photon will be trapped by the wake field if  $\Omega_0 < \Omega < \Omega_x$ , where the values for the Hamiltonian  $\Omega$  corresponding to the elliptic fixed point and to the separatrix are determined by

$$\Omega_0 = \frac{\omega_{p0}}{\gamma} \sqrt{1 - \epsilon a}, \quad \Omega_x = \frac{\omega_{p0}}{\gamma} \sqrt{1 + \epsilon b}. \quad (4)$$

When trapping occurs, the photon wave number  $p$  will oscillate between a minimum  $p^-$  and a maximum  $p^+$ , determined by

$$p^\pm = \gamma^2 \frac{\Omega}{c} \left\{ \beta \pm \left[ 1 - \frac{\omega_{p0}^2}{\gamma^2 \Omega^2} (1 + \epsilon f^\pm) \right]^{1/2} \right\}. \quad (5)$$

The maximum difference between these two extreme values can only be attained at the separatrix, for  $\Omega = \Omega_x$ , and it is given by

$$\Delta p_{\max} = 2\gamma \frac{\omega_{p0}}{c} \sqrt{\epsilon(a + b)}. \quad (6)$$

The corresponding maximum frequency shift which can be expected for the photon is then given by  $\Delta\omega_{\max} \simeq c \Delta p_{\max}$ , for  $\omega_i \gg \omega_{p0}$ . This result shows that  $\Delta\omega_{\max}$  is insensitive to the exact shape of the wake-field potential, and can be very large when  $v \rightarrow c$ , even for small values of  $\epsilon$ . In Fig. 1 we illustrate the photon dynamics in a wake field, for  $f(k_p \eta) = \cos(k_p \eta)$ . Three different trajectories in phase space  $(\eta, p)$  are shown in Fig. 1(a). The corresponding frequency shifts, as measured in the laboratory frame, are shown in Fig. 1(b). The largest frequency shift occurs for the trajectory closest to the separatrix and can be estimated by Eq. (6). Figure 1 also illustrates how easily the Hamiltonian approach to photon dynamics can be used for experimental modeling.

Let us now consider a more complicated, but not unrealistic situation, where the photons travel in a plasma modulated by two different wake fields. In this case, Eq. (3) is replaced by

$$\omega_p^2(\eta) = \omega_{p0}^2 [1 + \epsilon_1 \cos(\mathbf{k}_1 \cdot \boldsymbol{\eta}) + \epsilon_2 \cos \mathbf{k}_2 \cdot (\boldsymbol{\eta} - \mathbf{V}t)], \quad (7)$$

where  $\boldsymbol{\eta} = \mathbf{r} - \mathbf{v}_1 t$ ,  $\mathbf{V} = \mathbf{v}_1 - \mathbf{v}_2$ , and  $\mathbf{v}_j$  and  $\mathbf{k}_j$  are the velocities and wave vectors of the two wake fields. In Eq. (2),  $\mathbf{v}$  should now be replaced by  $\mathbf{v}_1$ . Here we have assumed the simplest possible wake field, with no harmonic content, but this will not change the qualitative properties of the resulting photon dynamics and will not affect the calculated frequency shifts.

Returning to the one-dimensional analysis, we now have two different nonlinear resonances in phase space, similar to the time-perturbed asymmetric pendulum [9]. The location  $p_i$  and half-width  $\Delta p_i$  of these two resonances are given by

$$p_i = \frac{\omega_{p0}}{c} \beta_i \gamma_i \sqrt{1 - \epsilon_i}, \quad \Delta p_i = \frac{\omega_{p0}}{c} \gamma_i \sqrt{2\epsilon_i}. \quad (8)$$

It is well known [10] that a transition to large scale sto-

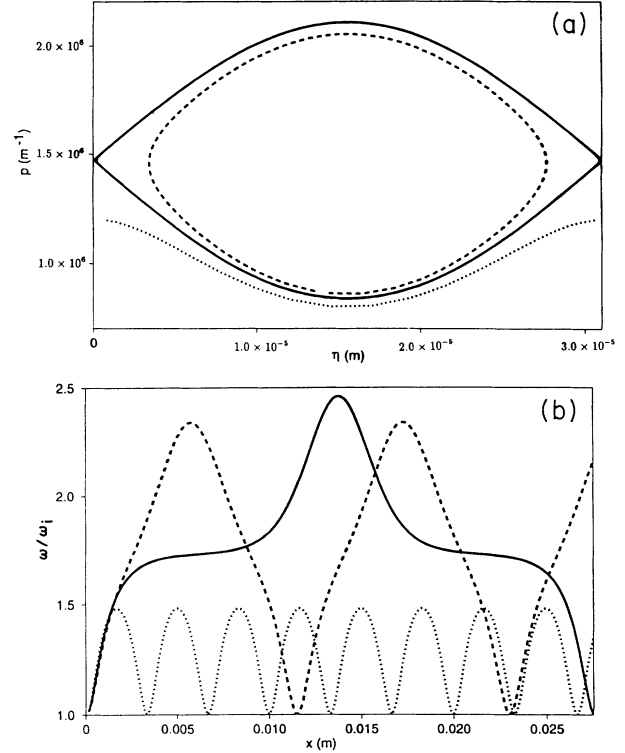


FIG. 1. (a) Phase space  $(\eta, p)$  of a photon interacting with a plasma wave wake field ( $\omega_{p0} = 6 \times 10^{13}$  Hz,  $\epsilon = 0.1$ ,  $\beta = 0.99$ ), for three different initial conditions:  $k_0 = 8 \times 10^5$  m $^{-1}$  (dotted line),  $k_0 = 8.3805 \times 10^5$  m $^{-1}$  (solid line), and  $k_0 = 8.6 \times 10^5$  m $^{-1}$  (dashed line), for the same  $\eta_0 = \pi/k_p$ ; (b) Space variation of the relative frequency shift, for the same photon trajectories.

chasticity can eventually occur, when the amplitude perturbations  $\epsilon_i$  attain a given threshold. When  $\epsilon_1 \simeq \epsilon_2$ , we can estimate this threshold with the aid of the overlapping criterion, which states that  $\Delta p_1 + \Delta p_2 \geq |p_2 - p_1|$ . This is equivalent to

$$\frac{\gamma_1 \sqrt{2\epsilon_1} + \gamma_2 \sqrt{2\epsilon_2}}{|\beta_2 \gamma_2 \sqrt{1 - \epsilon_2} - \beta_1 \gamma_1 \sqrt{1 - \epsilon_1}|} \geq 1. \quad (9)$$

It is important to note that such criterion is independent of the unperturbed plasma frequency and that it can be quite easily attained, even for  $\epsilon_1 \ll 1$ . In this case, corresponding to small density perturbations, Eq. (9) reduces to  $\epsilon_1 \geq (1 - \nu)^2/2$ , for  $\epsilon_2 \simeq \epsilon_1$ ,  $\beta_i \sim 1$  and  $\nu = \gamma_1/\gamma_2 \simeq 1$ . For illustration we give, in Fig. 2, an example of stochastic photon acceleration, where a large frequency spectrum with  $\Delta\omega/\omega_i \simeq 5$  was generated in a very short length scale ( $\Delta x < 10$  cm, in the laboratory frame) starting from a nearly monochromatic wave packet,  $\Delta\omega_i \simeq 0$ .

We now turn to the case of photon interaction with an ionization front. Again, we make use of the dynamical Eqs. (1) and (2), but now we use

$$\omega_p^{(2)}(\eta) = \omega_{p0}^2 \tanh(\mathbf{k}_f \cdot \boldsymbol{\eta}), \quad (10)$$

where  $\mathbf{k}_f$  gives the front length (or time) scale, and  $\omega_{p0}$  is the asymptotic value attained by the plasma frequency well behind the ionization front.

Let us assume a photon initially propagating in the

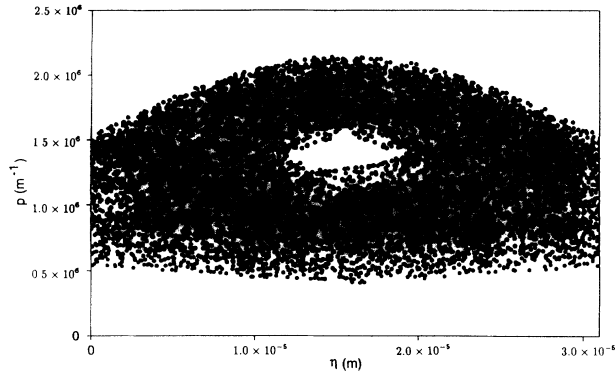


FIG. 2. Poincaré surface of section of a single-photon trajectory moving in presence of two plasma wave wake fields ( $\omega_{p0} = 6 \times 10^{13}$  Hz,  $\epsilon_1 = \epsilon_2 = 0.1$ ,  $\beta_1 = 0.99$ ,  $\beta_2 = 0.97$ ). Initial conditions:  $k_0 = 8.37 \times 10^5$  m $^{-1}$  and  $\eta_0 = 0$ .

neutral gas region, far away from the ionization front. If we neglect the dispersion properties of the gas we can write  $\Omega = \omega_i(1 + \beta)$ , when  $\mathbf{k}_i$  is antiparallel to the front velocity  $\mathbf{v}$ . Using the invariance of  $\Omega$ , we can then say that the final or asymptotic value for the photon frequency,  $\omega_f$ , after collision with the ionization front, will simply be

$$\omega_f = \frac{\Omega}{1 - \beta} = \omega_i \frac{1 + \beta}{1 - \beta}. \quad (11)$$

This is the simplest possible derivation of the well-known relativistic mirror effect. If the neutral gas region is replaced by a weakly ionized plasma, with a plasma density lower by a factor  $\delta \ll 1$  than that produced by the ionization front, the parameter  $\beta$  in Eq. (11) will be multiplied by a factor  $(1 - \delta)^{1/2}$ . This agrees with the result recently obtained by Kaw, Sen, and Katsouleas [11].

Using the same kind of arguments it is also easy to calculate the frequency shift which occurs when the photon crosses over the ionization front without reflection. For  $\omega_i \gg \omega_{p0}$ , we obtain, in this case:  $\Delta\omega = (\omega_{p0}^2 / 2\omega_i) \{ \beta / (1 \pm \beta) \}$ , where the signs + (respectively, -) pertains to the antiparallel (respectively, parallel) propagation. We see that the frequency shift can still be quite large, for parallel propagation, but smaller by a factor of order  $(\omega_{p0} / \omega_i)^2$  than in the case of reflection.

It is now important to determine the conditions for which photon reflection takes place. Two different reflection conditions can be defined for antiparallel propagation. If we look at the phase-space dynamics of the photon trajectories, we can say that the condition for the photon to reverse its way along the  $\eta$  axis is the existence of an  $\eta$  turning point, corresponding to  $(\partial p / \partial \eta) \rightarrow -\infty$ . Such a turning point exists for initial photon frequencies smaller than a given cutoff frequency  $\omega_\eta$ , to be defined below.

On the other hand, we can say that photon reflection occurs on real space if there is an  $x$  turning point such that  $p \equiv k = 0$ . This occurs for  $\omega_i < \omega_x$ , where  $\omega_x$  is another cutoff frequency. These two cutoff frequencies can be very easily derived from Eqs. (1), (2), and (10), and are determined by

$$\omega_x = \frac{\omega_{p0}}{1 + \beta} = \gamma \omega_\eta. \quad (12)$$

When the velocity of the ionization front tends to zero,  $\beta \rightarrow 0$ , they tend to the plasma frequency  $\omega_{p0}$ , as expected. But the existence of two distinct cutoffs, for  $\beta \neq 0$ , leads to three different kinds of trajectories for antiparallel propagation, which are illustrated in Fig. 3(a).

Trajectories of kind I, corresponding to  $\omega_i > \omega_x$ , are only slightly perturbed by the front and always take positive values for the wave number  $p$ . Trajectories of kind II, existing in the interval  $\omega_x > \omega_i > \omega_\eta$ , are reflected in real space but have no turning point in phase space. The frequency shift is now larger than for kind I, but it remains small. Finally, for  $\omega_i < \omega_\eta$ , we have reflection in both spaces (phase space and real space). The frequency shift now attains its largest possible value, given by Eq. (11).

The frequency shifts corresponding to these three trajectories are given in Fig. 3(b). It is important to note that the final photon frequency is independent of the slope  $k_f$  of the ionization front. This can be an important property to take into account when designing photon acceleration experiments. For instance, trajectory of kind III shows that a significant frequency shift can occur within 1 m, for a relatively slow time constant for the

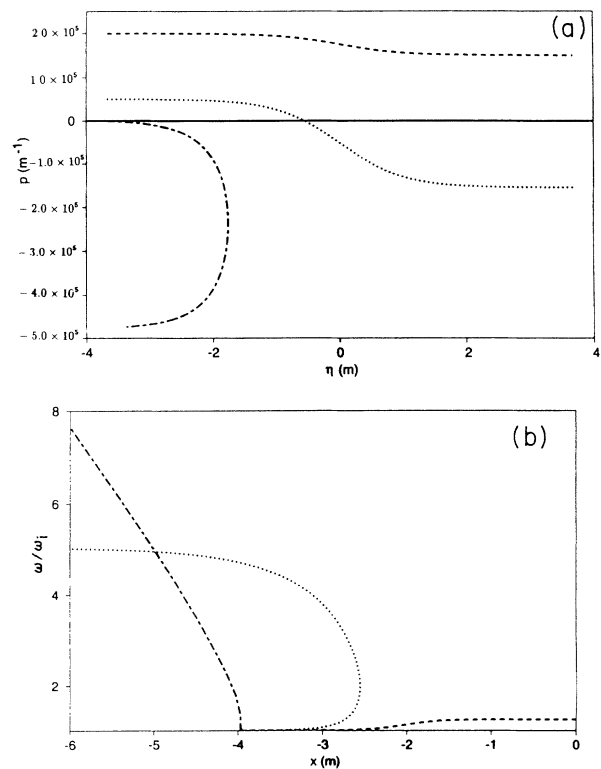


FIG. 3. (a) Phase space ( $\eta, p$ ) of a photon interacting with a moving ionization front ( $\omega_{p0} = 6 \times 10^{13}$  Hz,  $\beta = 0.99$ ,  $k_p = 1$  m $^{-1}$ ) for three different initial conditions: (I)  $k_0 = 2 \times 10^5$  m $^{-1}$  (dashed line); (II)  $k_0 = 5 \times 10^5$  m $^{-1}$  (dotted line); and (III)  $k_0 = 10^5$  m $^{-1}$  (double dotted line), for the same  $\eta_0 = -3.6$ ; (b) Space variation of the relative frequency shift, for the same photon trajectories.

ionization front (3 ns). The existence of three kinds of trajectories were recently suggested by Mori [2] and by Yu *et al.* [6], using a different and less explicit approach.

In conclusion, we have shown how the various mechanisms of photon acceleration could be described using the Hamiltonian formulation of the ray tracing equations. The resulting calculations are simple and exact, leading to precise estimates of the maximum possible frequency shifts and of the involved time and length scales. In particular, it was demonstrated that large frequency shifts can be attained within a 1-m length, using relatively slowly growing ionization fronts (a few nanoseconds). The existence of three different kinds of photon trajectories was also clearly demonstrated on topological grounds, for

photon interaction with an ionization front. Another important result was the demonstration of a transition from regular to stochastic photon acceleration, in the case of photon interaction with two different wake fields, within not too stringent conditions. This opens the way for future generation of white light, starting from nearly monochromatic radiation.

One of the authors (J.T.M.) would like to acknowledge stimulating discussions with Professor J. M. Dawson, as well as with Bob Bingham and David Resendes, which were the starting point of the present work. This work was supported by JNICT, STRIDE, and FEDER under Contract No. STRD/C/FAE/1012/93.

- 
- [1] V. I. Semanova, *Sov. Radiophys.* **10**, 599 (1967); M. Lampe, E. Ott, and J. H. Walker, *Phys. Fluids* **21**, 42 (1978).
- [2] P. Sprangle, E. Esarey, and A. Ting, *Phys. Rev. A* **41**, 4463 (1990); H. C. Kapteyn and M. M. Murnane, *J. Opt. Soc. Am. B* **8**, 1657 (1991); W. B. Mori, *Phys. Rev. A* **44**, 5118 (1991); R. L. Savage, Jr., C. Joshi, and W. B. Mori, *Phys. Rev. Lett.* **68**, 946 (1992).
- [3] J. T. Mendonça, *J. Plasma Phys.* **22**, 15 (1979).
- [4] S. C. Wilks, J. M. Dawson, W. B. Mori, T. Katsouleas, and M. E. Jones, *Phys. Rev. Lett.* **62**, 2600 (1989).
- [5] R. L. Savage, Jr., R. P. Brogle, W. B. Mori, and C. Joshi, *IEEE Trans. Plasma Sci.* **21**, 5 (1993).
- [6] W. Yu, J. Ma, Z. Xu, and Z. Sheng, *Phys. Rev. A* **46**, 8021 (1992).
- [7] S. Weinberg, *Phys. Rev.* **126**, 1899 (1962); I. B. Bernstein and L. Friedland, in *Handbook of Plasma Physics*, edited by M. N. Rosenbluth and R. Z. Sagdeev (North-Holland, Amsterdam, 1983), Vol. 1.
- [8] J. M. Rax and N. J. Fisch, *Phys. Fluids B* **4**, 1323 (1992); R. Bingham, V. de Angelis, M. R. Amin, R. A. Cairns, and B. McNamara, *Plasma Phys. Controlled Fusion* **34**, 557 (1992).
- [9] L. Oliveira e Silva and J. T. Mendonça, *Phys. Rev. A* **46**, 6700 (1992).
- [10] A. J. Lichtenberg and M. A. Lieberman, *Regular and Stochastic Motion* (Springer-Verlag, Berlin, 1989).
- [11] P. K. Kaw, A. Sen, and T. Katsouleas, *Phys. Rev. Lett.* **68**, 3172 (1992).